FINAL REPORT

PROJECT FIRE MODEL

AN EXPERIMENTAL STUDY OF MODEL FIRES

by

G. M. Byram

H. B. Clements

M. E. Bishop

R. M. Nelson, Jr.

for

OFFICE OF CIVIL DEFENSE
OCD-PS-65-40

through

National Bureau of Standards
U. S. Department of Commerce
Washington, D. C. 20234

NBS Purchase Order No. S-302190-62-63 and Supplements

with

Forest Service, U. S. Department of Agriculture
Southeastern Forest Experiment Station
Southern Forest Fire Laboratory
P. O. Box 236
Macon, Georgia 31202

June 1, 1966

DISTRIBUTION OF THIS DOCUMENT IS UNLIMITED

ACKNOWLEDGMENT

This work was supported in part by the Office of Civil Defense and through contract with the National Bureau of Standards. It is in the public domain and not subject to copyright.

Acknowledgment is made to the Georgia Forest Research Council for making facilities available. Credit is due P. M. George, R. K. Burgess, A. T. Jackson, and Kelly Mink for their assistance in the experimental work and reduction of data and for their effective efforts in the construction of special equipment needed for some of the test fires.

TABLE OF CONTENTS

AN EXPERIMENTAL STUDY OF MODEL FIRES

INTRODUCTION

Modeling has long appeared to be one of the most promising methods for studying the spread and behavior of free-burning fires but progress in the use of models for predicting the behavior characteristics of full-scale fires has been slow. Possibly this has been due to the lack of knowledge of the basic physical mechanisms of fire spread and to uncertainty as to the relative significance of the many variables (probably about thirty) which enter the problem of fire spread.

The main objectives of the experimental work described in this report were (1) to gain more knowledge of the structure of free-burning fires, (2) to obtain a better understanding of the mechanisms of fire spread, and (3) to determine the significance of some of the many independent variables in fire spread. Although it was not possible to predict the behavior of large-scale fires from the crib and pool fires used in this study, the information gained from these tests was essential for work now underway in the development of scaling laws and in determining the characteristics that a model fire should have.

This report will deal primarily with the physical characteristics such as rate of spread, fuel burning rate, flame length, flame temperature, and flame velocity of crib and pool fires. It will also consider the possible effects of wind speed and slope on the residence

time and the unit area burning rate--two basic fuel bed parameters. Some results of work now in progress on scaling law development will be summarized briefly.

FLAME CHARACTERISTICS

The flame zone may be regarded as the lower part of the convection column which is in contact with the burning fuel and the earth's surface. It is also the space in which most of the energy-releasing combustion process takes place. The rate of spread of most fires is largely determined by the properties and characteristics of the flame zone.

Fifteen ethanol pool fires were burned in a wind tunnel[1/] in order to investigate the effect of wind speed and pool size on the shape and structure of the flame zone. Wind speeds of 2, 4, 6, 8, and 10 ft/sec were used for each of the three different pool sizes. The pool dimensions in the direction of the airflow were 2.5, 5.0, and 12.8 inches. All three pools were 12.8 inches long and 1.25 inches deep. Placed parallel to the direction of airflow, 2 x 4-foot glass panels on both sides of the pool gave the fires the characteristics of infinite length.

For a fire burning in calm air and on a horizontal surface, the flames have a tendency to tilt toward the fire center from all

---

1/ This wind tunnel was described by Byram et al. (1964) in Technical Report No. 3.

sides. However, even a light wind causes the fire to undergo a marked change from its calm air form. The inertial forces of the wind stream displace and elongate the flame so that it is in nearly continuous contact with the horizontal surface for some distance beyond the downwind side of the burning pool. A vertical cross section of the flame zone for a fire in wind is shown in the drawing of Figure 1. The cross section is parallel to the direction of wind flow.

Two types of indicators were used to show contact of flame with the horizontal surface beyond the area of burning fuel. One was a layer of brown paper, coated with diammonium phosphate, which covered the table surface beyond the burning pool on its downwind side. The flame-proofed paper served as an indicator of continuous flame contact. The other type of indicator consisted of a series of small loose cotton tufts located about one-half inch above the table downwind from the fire on a line passing through the fire center. Spaced two inches apart, these tufts served as indicators of flame contacts of very short duration.

It was assumed that the distance of continuous flame contact, or scorch distance, beyond the downwind edge of the burning fuel could be determined by measuring the length of the scorched area on the brown paper. Figure 2 shows this distance plotted as a function of wind speed for different pool widths. Beyond the distance of continuous flame contact with the horizontal surface (as indicated by the scorched area of the paper) the flames curved upward into the

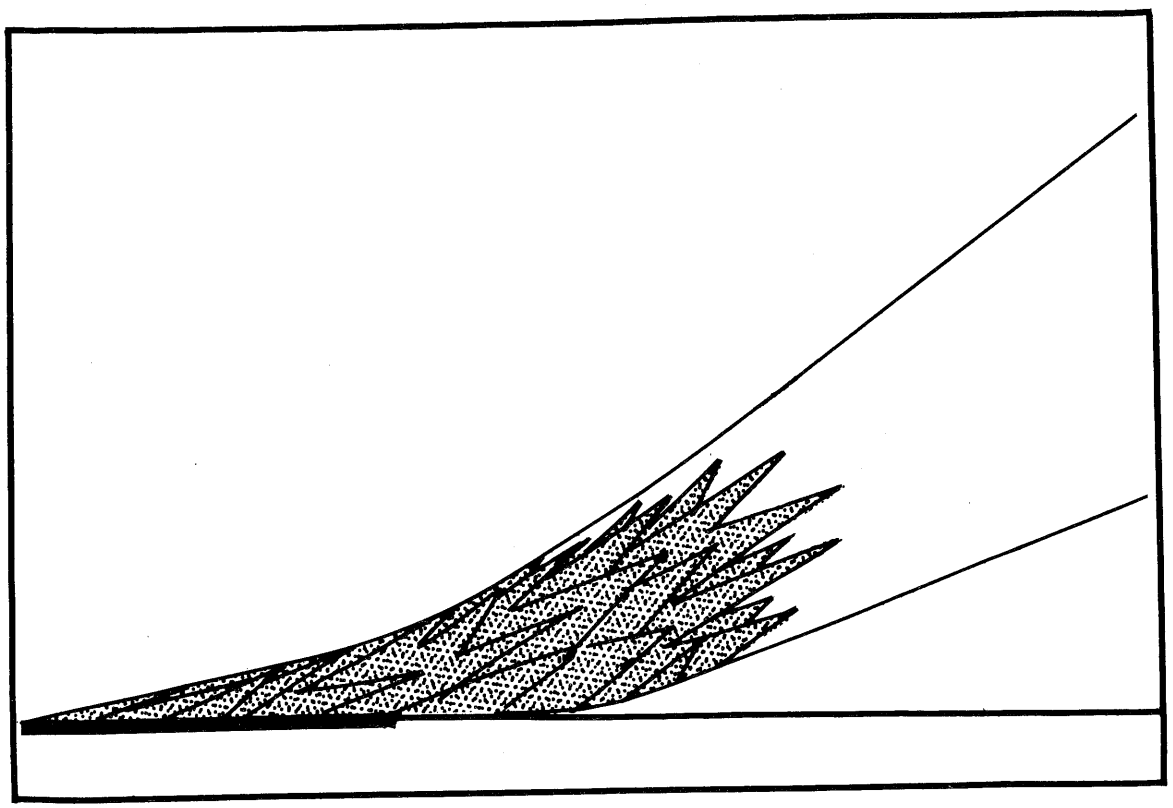

Figure 1.--A vertical cross section of the flame zone and lower convection column is shown for a fire over a pool of burning ethanol in the presence of a light wind. The pool width is indicated by the heavy horizontal line.

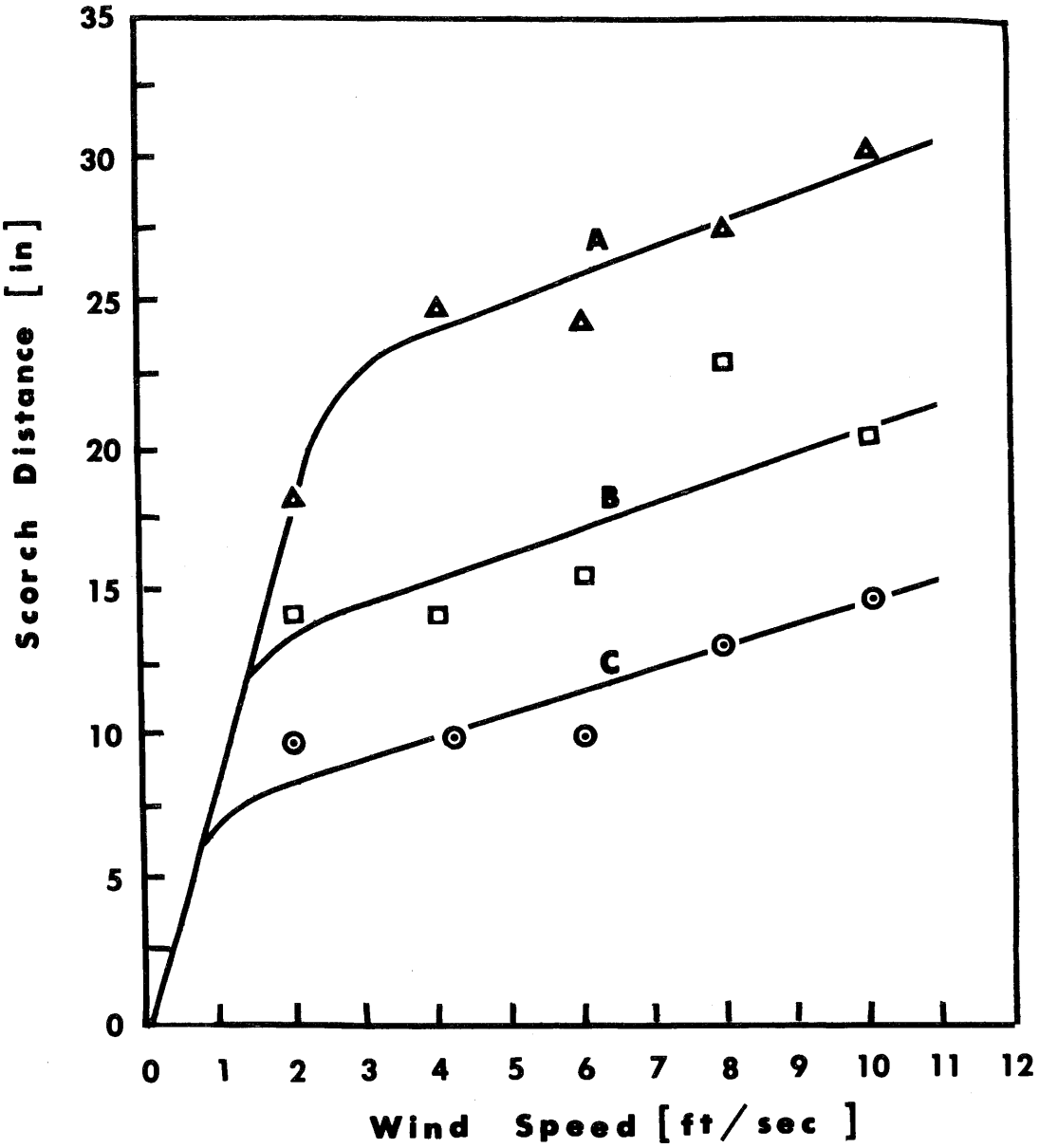

Figure 2.--The scorch distance is shown as a function of wind speed for pools of burning ethanol with widths of 12.8 inches (curve A), 5.0 inches (curve B), and 2.5 inches (curve C).

convection column. However, beyond this area, turbulent fingers of flame would dart downward, apparently at random, from the main body of flame to make intermittent contacts with the surface. This intermittent contact distance or ignition distance was determined by measuring the distance between the downwind edge of the burning pool and the most distant burned cotton tuft. The distance increased with increasing wind speed and increasing pool width as shown in Figure 3. Owing to the presence of the glass panels, the height of this curve is considerably greater than that for a similar curve for the same heat source given in Technical Report No. 3 by Byram et al. (1964).

The horizontal component of the flame length, as measured from the center of the burning area, was determined photographically. Figure 4 shows that the horizontal component of flame length varies with wind speed and pool width in much the same manner as do the two flame contact distances.

The flames over a burning area on a plane sloping surface are displaced and elongated in the upslope direction in much the same way that flames are influenced by wind on a horizontal surface; the upslope component of buoyancy of the hot flame gases has an effect on the flame zone similar to that of the inertial forces in a wind stream. The flame displacement process appears to be a key part of the spread mechanism for slope-driven and wind-driven fires in solid fuels as was pointed out by Byram et al. (1964). It may play a considerably more important part in fire spread than does radiation from the flames above the fuel. Ignition of fresh surface fuel by

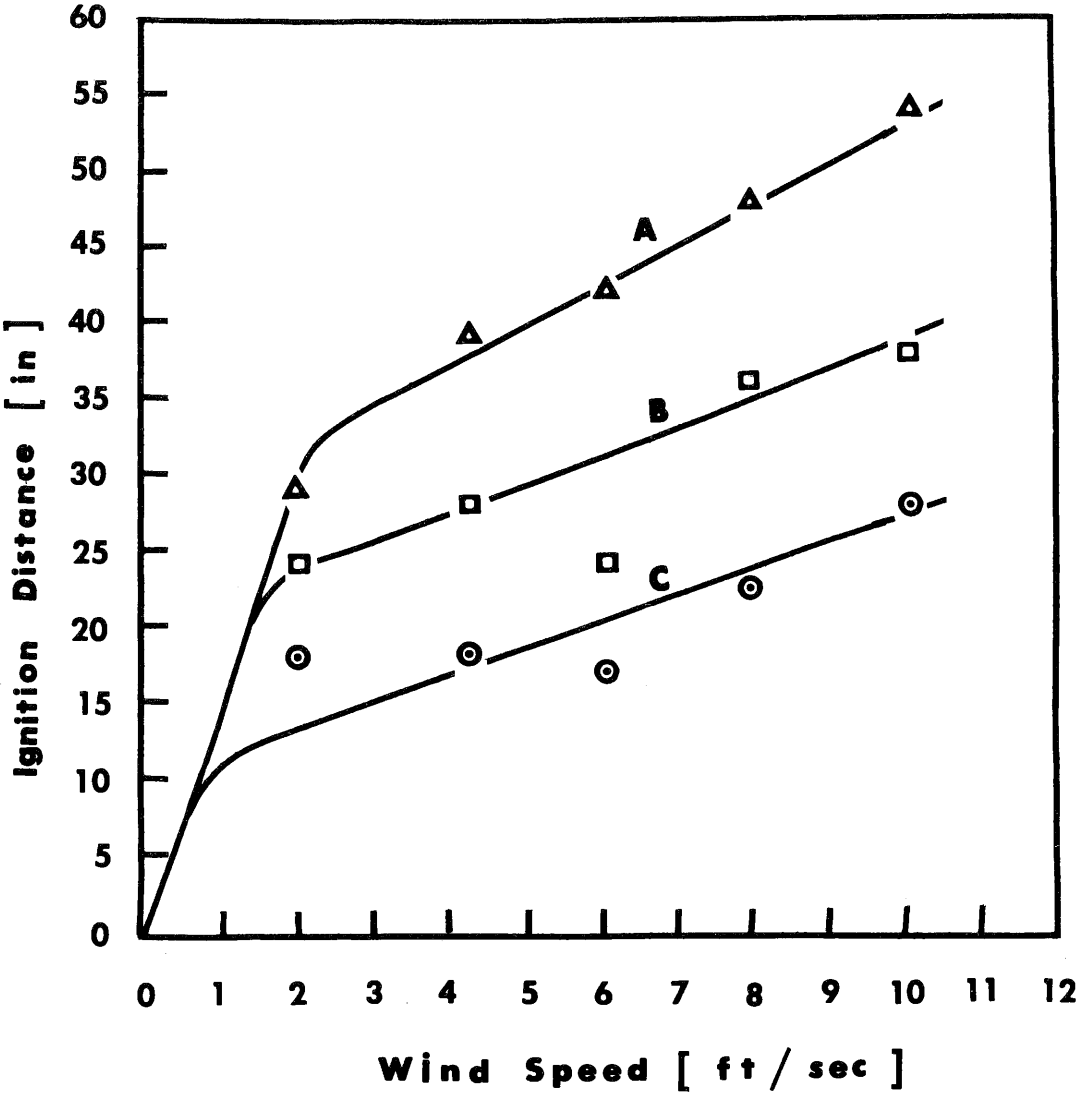

Figure 3.--The intermittent flame contact distance as indicated by the flaming of cotton tufts is shown as a function of wind speed for pools of ethanol with widths of 12.8 inches (curve A), 5.0 inches (curve B), and 2.5 inches (curve C).

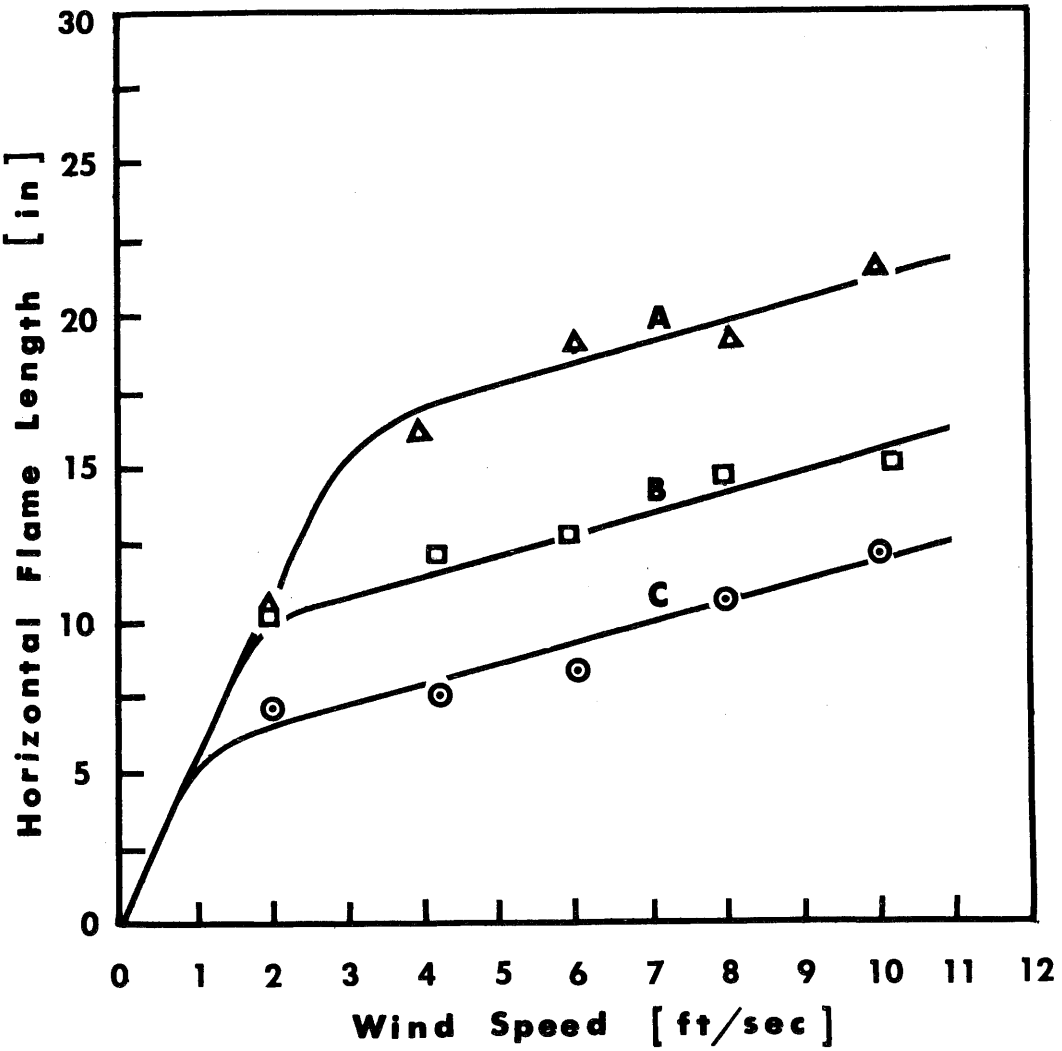

Figure 4.--The horizontal component of flame length for pools of burning ethanol is shown as a function of wind speed for pool widths of 12.8 inches (curve A), 5.0 inches (curve B), and 2.5 inches (curve C).

convective heat transfer from the displaced flames should be dependent on both the temperature and velocity of the flames. The burning rates for the pool fires were not greatly affected by wind speed for the 2.5-inch and 5.0-inch pools but decreased with increasing wind speed for the 12.8-inch pool. Data for these fires are given in Table 1 in Appendix B.

For many years flame temperatures of 1600 to 1800°F have been reported in the literature for fires burning in woody fuels. However, most of these temperature measurements have been made on small fires with small flames. In such fires the indicated thermocouple temperature may be considerably less than the actual flame temperatures because of radiative heat loss from the thermocouple junction. If fine wires are used in constructing the thermocouple, the heat loss by conduction through the leads is small compared to the loss due to radiation.

If radiation accounts for most of the heat loss from the thermocouple junction, it is not difficult to estimate the true flame temperature from the thermocouple reading and a measurement of the gas velocity in the vicinity of the thermocouple junction. Curve A in Figure 5 shows the central temperature at different heights over a 12.8-inch pool[2/] of burning ethanol as indicated by the thermocouple readings and curve B is the corrected curve. Corrections were based

---

2/ It was simpler to use a different fire for each pair of temperature and flame velocity measurements than to obtain all measurements on a single fire.

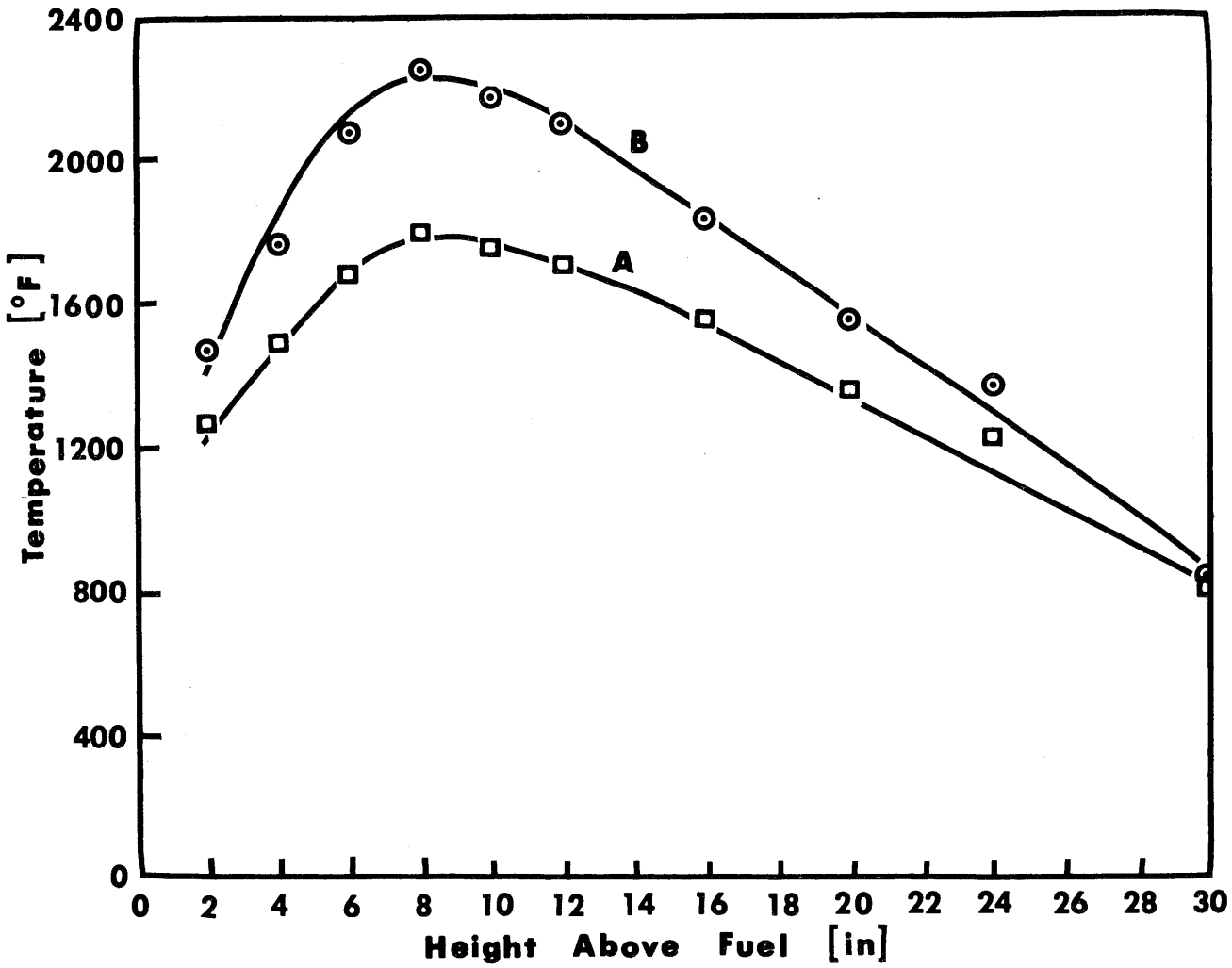

Figure 5.--The central flame temperature as indicated by a thermocouple (curve A) is shown as a function of the distance above the surface of a 12.8-inch pool of ethanol burning in calm air. Curve B is the corresponding curve after corrections have been made for the thermocouple radiation loss and central vertical gas velocity.

on the thermocouple readings and the associated flame or gas velocity. This velocity was determined by a 1/8-inch stainless steel Prandtl tube located near the chromel-alumel thermocouple junction, which was 0.013 inch in diameter. The procedure for making the temperature correction is given in more detail in Appendix A and the data for the correction are presented in Table 2 of Appendix B. Table 3 gives similar data for fires in white fir cribs (Abies concolor) 11.6 inches square and 1.56 inches high.

WIND AND FIRE SPREAD

Anyone who has observed fire spreading in forest fuels can readily appreciate the influence of wind on rate of fire spread. The most obvious effect of wind is in the tilting of the flames toward the unburned fuel. This change in the flame front should increase the radiation received by the surface of the unburned fuel layer ahead of the spreading fire and it has been assumed by some investigators that this increase in radiation intensity may explain the effect of wind on the rate of fire spread. Although radiation from the flames is undoubtedly a factor in the continuing ignition of the surface fuel ahead of an advancing fire, its effect is probably small compared to that resulting from the contact and envelopment of the surface fuels by the flames displaced horizontally by the wind stream. The continuing ignition of new surface fuel at the flame front and the eventual burnout of fuel at any given point in the burning zone as the fire progresses results in the sloping layer of burning fuel illustrated

by the simplified vertical cross section ABCD shown in Figure 6. The line AB represents the front surface of this layer, which may be defined as the ignition surface. In the steady state this surface moves in the direction of fire spread at the same speed as the rate of spread R. If R' is the speed at which this surface moves into the unburned fuel, then

$$R' = R \sin\theta$$

where θ is the angle between the ignition surface and the horizontal. For crib fires in calm air, or for fires spreading against the wind, the angle θ is in the neighborhood of $\pi/2$ and in these cases R' and R are about equal. However, for a fire burning in only a light wind, R is much greater than R' and θ is small.

The burning zone ABCD is the region in which the volatile fractions are distilled and the residual solid fuel burned. The volatiles are burned in a region most of which is located above the fuel bed. This region is defined as the flame zone. The residual solids (charcoal) are burned in the trailing side of the zone ABCD.

The effect of wind on fire spread has been studied by a number of investigators but no definite relationship between rate of fire spread and wind has yet been determined. The results of Anderson and Rothermel (1965) for fires burning in beds of pine needles indicate that rate of spread varies with some power of wind speed greater than the first, at least for wind speeds up to about 12 ft/sec. The early results of Fons (1946) for the same fuel gave curves resembling those of Anderson and Rothermel. In Technical Report No. 3, the results of

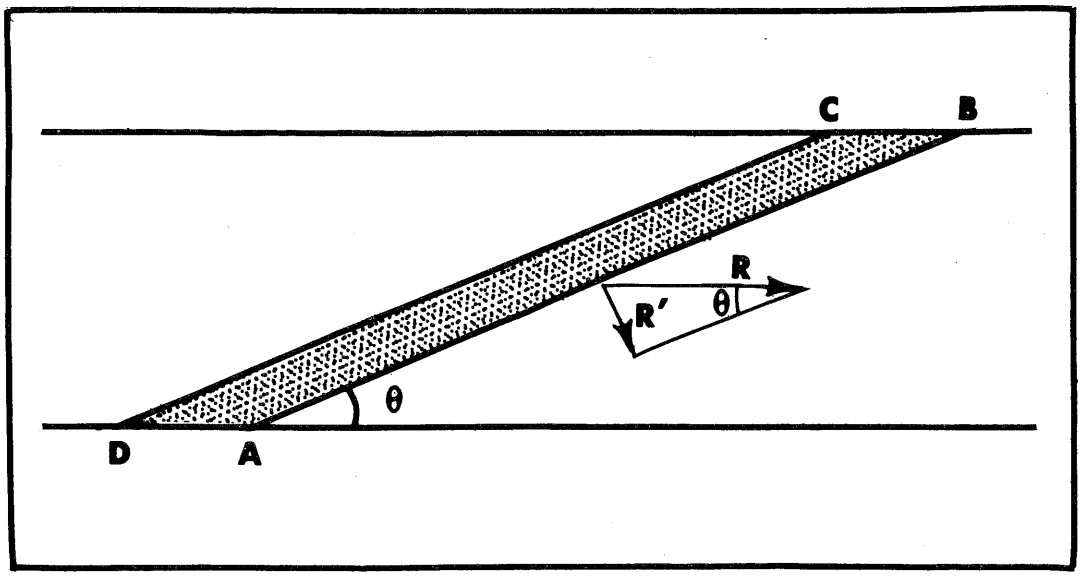

Figure 6.--A vertical cross section of the fuel bed and burning zone ABCD for a wind-driven fire spreading in a bed of solid fuel. The cross section is parallel to the direction of the wind and fire spread.

Byram et al.(1964) for wood cribs weighing from 0.57 to 1.37 lb/ft^2 indicated a linear relationship between rate of spread and wind speed. However, they reported that steady-state burning was not attained because of inadequate crib length.

In the present study of the effect of wind on fire spread, the cribs had a considerably smaller height-to-width ratio and weighed 0.57 lb/ft^2. They were made up in 3- and 6-foot sections to permit lengths in multiples of 3 feet to be fitted together and burned as one long crib. The crib sections were made up of 1/4-inch white fir sticks for which the average density of the wood was 25.6 lb/ft^3. The lateral spacing of the sticks was 1.0 inch. The cribs were 1.56 inches high and 11.6 inches wide and conditioned in a constant-humidity cabinet to a moisture content of about 10.8 percent. Strips of brown paper treated with diammonium phosphate were glued to the sides of the cribs to prevent air from entering through the sides.

Tests with both headfires (fires burning with the wind) and backfires (fires burning against the wind) were made in the low-speed wind tunnel described in Technical Report No. 3. Headfires were burned with wind speeds of 2, 3, 5, 8, 10, and 12 ft/sec and backfires with wind speeds of 2, 5, 8.5, and 12 ft/sec. The average temperature of the air was about 73°F for the tests and the relative humidity was between 54 and 62 percent. A special combustion table was constructed for burning the long cribs (up to 21 feet) required to obtain steady-state burning for the headfires. The body of the 2 x 18-foot table consisted of an inner rectangular frame of 1 x 4-inch boards covered

on the top and bottom with 1/4-inch plywood sheets. A 5-inch diameter steel cylindrical roller with bearings was installed at each end of the table. A continuous belt of fiberglass cloth was made to fit over the table and rollers. One roller was covered with a rubber traction material to prevent slippage of the conveyer belt. A chain gear drive mechanism was connected to this same roller so the belt could be moved by a hand-operated crank. The table was installed in the test section of the wind tunnel and a 3/4-inch steel shaft was used to connect the chain drive mechanism to a hand crank outside the tunnel. One revolution of the hand crank moved the belt 3.14 inches. A 1/2-inch layer of vermiculite insulated the belt and table from the crib fires.

The fires were started by igniting a gasoline-soaked asbestos wick in a shallow trough placed under one end of the crib. During ignition it was necessary to shield the crib from the wind for a short time until the flames in the crib were well established.

To assure sufficient crib length for steady-state burning at high wind speeds, extra crib sections were added during the burning tests as needed. The conveyer belt was moved at a rate which kept the burning zone approximately fixed in the test section of the tunnel. The rates of spread of the front and rear of the flames were measured visually. Conditions and results of the fires are given in Table 4 of Appendix B. In Figure 7 the rate of spread is shown as a function of wind speed. The headfire curve (curve A) resembles more the relationships obtained by Anderson and Rothermel (1965) and Fons (1946)

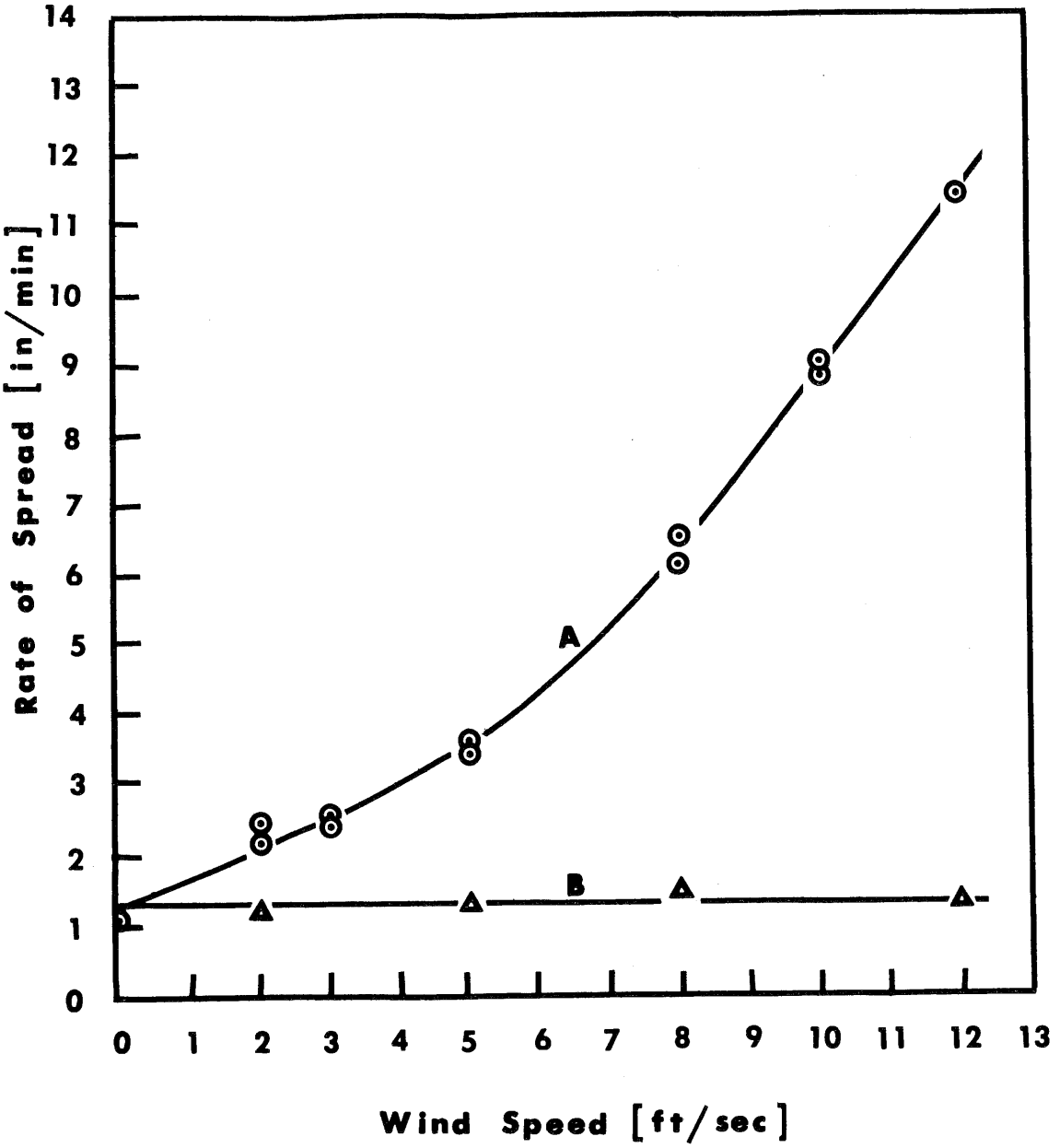

Figure 7.--The relation between rate of spread and wind speed is shown for headfires (curve A) and backfires (curve B) for fires burning in wood cribs 1.56 inches high and 11.6 inches wide constructed of 1/4-inch white fir sticks.

than it does the linear relationship for the cribs described in Technical Report No. 3. Apparently the shape of this curve depends on the crib or fuel bed structure and possibly on the attainment of steady-state conditions.

Curve B in Figure 7 indicates that wind has no appreciable influence on the rate of spread of crib backfires. The flames above the fuel bed probably have little influence on the spread of these fires. It is likely that radiative and conductive heat transfer within the fuel bed constitute the main spread mechanism.

In Figure 8 the flame zone width D_z is plotted against the rate of spread R for crib fires, which were burned in winds with speeds from 2 to 12 ft/sec. The curve drawn through the data is a straight line having a slope of 1.0 in the log-log plot. Thus at least for the type of wood crib used, the ratio D_z/R does not appear to depend on the wind speed. This ratio is the residence time t_r which Fons et al. (1962) defined as the time that a fuel particle spends in the flame; it can also be regarded as the burnout time for the fuel bed volatile fractions. Closely related to t_r is the variable τ which may be defined as the burnout time for all of the fuel bed fractions (including the residual charcoal); τ is given by the equation $\tau = D/R$ where D is the width of the burning zone. Although τ is probably a more significant variable than t_r, it is more difficult to determine, owing to the indefinite boundary of the charcoal in the trailing edge of the burning zone. Since τ and t_r are closely related and since t_r does not appear to depend on wind speed, then it is probable that τ may be but little affected by wind.

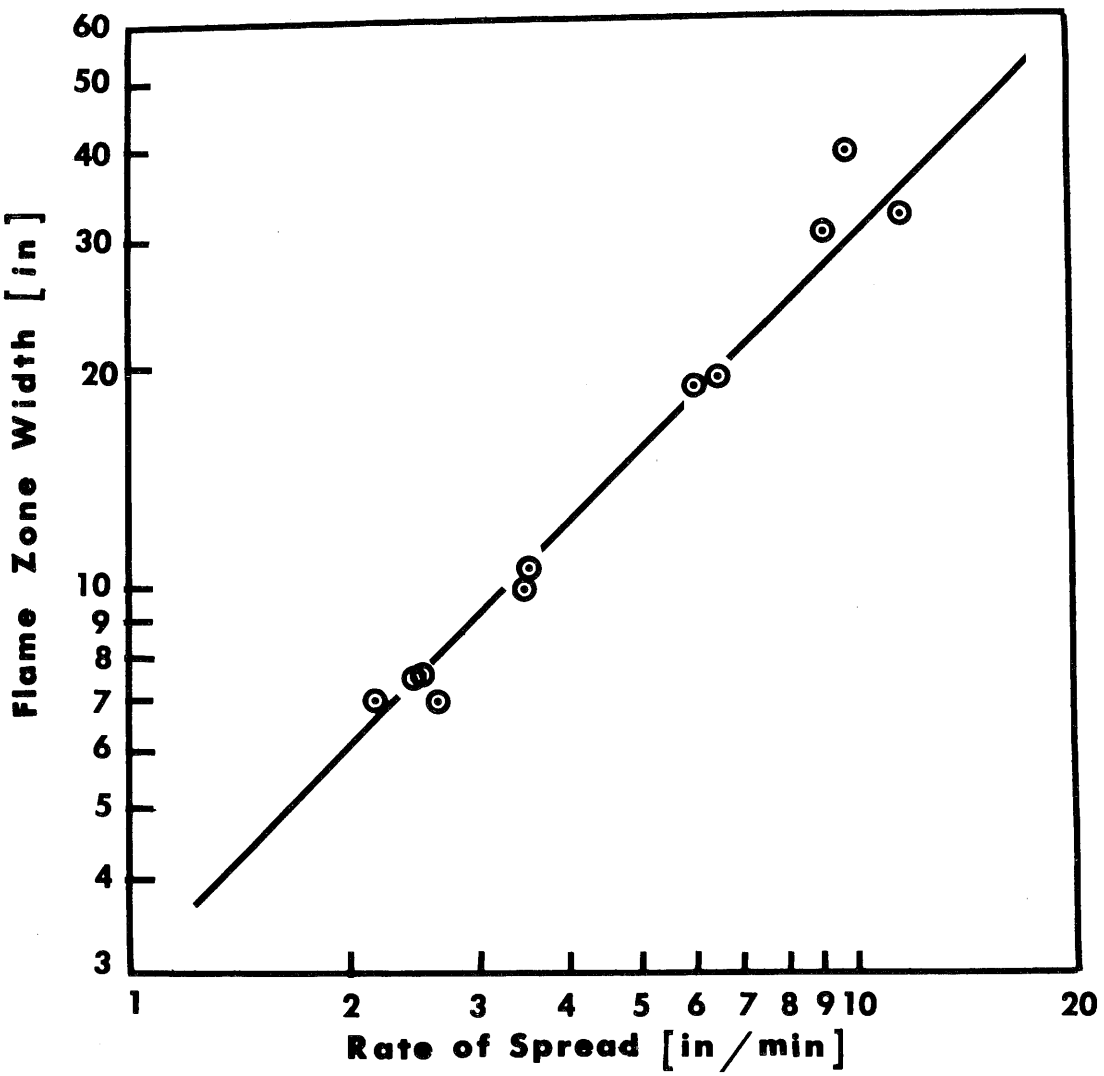

Figure 8.--The flame zone width D_z is shown as a function of the rate of spread R on a log-log plot for wood crib headfires in wind.

One of the basic variables of fire spread is the mean value of the unit area burning rate. This rate can be expressed either as G, the average rate of loss of mass per unit area of fuel bed, or as I_a, the average rate of convective heat output per unit area of fuel bed. These quantities are related by the equation

$$I_a = H_c G, \tag{1}$$

where H_c is the convective heat of combustion. For the burning zone, G and I_a are given by the relationships

$$G = W_a/\tau \tag{2}$$

and

$$I_a = H_c W_a/\tau \tag{3}$$

in which W_a is the loading, or mass of fuel per unit area.

For the flame zone, G and I_a are given by the equations

$$G = \frac{W_a - (H_c'/H_c)W_a'}{t_r} \tag{4}$$

and

$$I_a = \frac{H_c W_a - H_c' W_a'}{t_r} \tag{5}$$

in which H_c' is the heat of combustion of charcoal and W_a' the average mass of charcoal per unit area between the trailing edge of the flame zone and the trailing edge of the burning zone.

Since Figure 8 indicates that wind has but little effect on t_r, then one might conclude from Equations (4) and (5) that G and I_a should also be nearly independent of wind speed. Values of G and I_a based on

Equations (2) and (3) should also be independent of wind if τ is not dependent on wind. Equations (2) and (3) give smaller values of G and I_a than do Equations (4) and (5).

FIRE SPREAD ON A SLOPING SURFACE

The slope of the earth's surface in mountainous country has a marked effect on the rate of spread of free-burning fires. In the absence of wind, the rate of fire spread up a steep mountain slope may be many times as great as for a fire in the same fuel on level ground. Curry and Fons (1938) reported that the rate of fire spread in pine needles increases curvilinearly with slope. Murphy (1963) made similar observations for smoldering (no-flame) fires in thin layers of woodflour-sodium nitrate mixture.

The flame over a fuel bed burning on a sloping surface is displaced upslope along the surface and tilted toward the surface in the same manner as the flames for a wind-driven fire on the horizontal. The flames and hot gases have an upslope component of buoyancy which has much the same effect as the inertial forces in a wind stream for a fire on the horizontal, so the general mechanism of spread is similar in the two cases. The most important difference is that the component of buoyancy along the sloping surface increases with increasing fire intensity, whereas the inertial forces in a wind stream remain constant for a given wind speed. A slope-driven fire in heavy fuel can therefore build up very rapidly to a high rate of spread.

Wood crib fires were used to study the effect of slope on rate of spread for both upslope and downslope fires. The upslope fires correspond to the headfires in wind on a level surface and the downslope fires correspond to the backfires. The same type of crib sections, 3 and 6 feet in length, were used for the fires on slopes as for the fires in wind. The sloping surface on which the cribs were burned consisted of a tilted platform 12 feet long, 4 feet wide, and 3 1/2 inches thick. The platform was made by covering a rectangular frame of 1 x 3-inch boards with 1/4-inch plywood sheets. The top surface of the platform was also covered with a layer of 1/4-inch asbestos sheet held above the plywood by 1/4-inch spacers to reduce heat conduction to the plywood. Adjustable props were attached to the platform near one end, which allowed the cribs to be burned at angles of 0, 11.3, 21.8, 31.0, 38.7, 45, and 60 degrees with the horizontal. To prevent the crib and its charcoal remains from sliding down the slope, small wire nails were mounted in the asbestos sheet so that they protruded about 1/4-inch above the surface.

The crib fires were started by igniting an asbestos wick saturated with gasoline and placed beneath one end of the crib. Rates of spread of both the front and rear of the flame zone were determined visually. All fires reached steady-state burning conditions except one for which the slope was 60 degrees. In this case the front rate of spread was about twice the rear rate of spread. Figure 9 shows the rate of spread as measured visually for both upslope and downslope fires in the absence of wind. The rate of spread of upslope fires

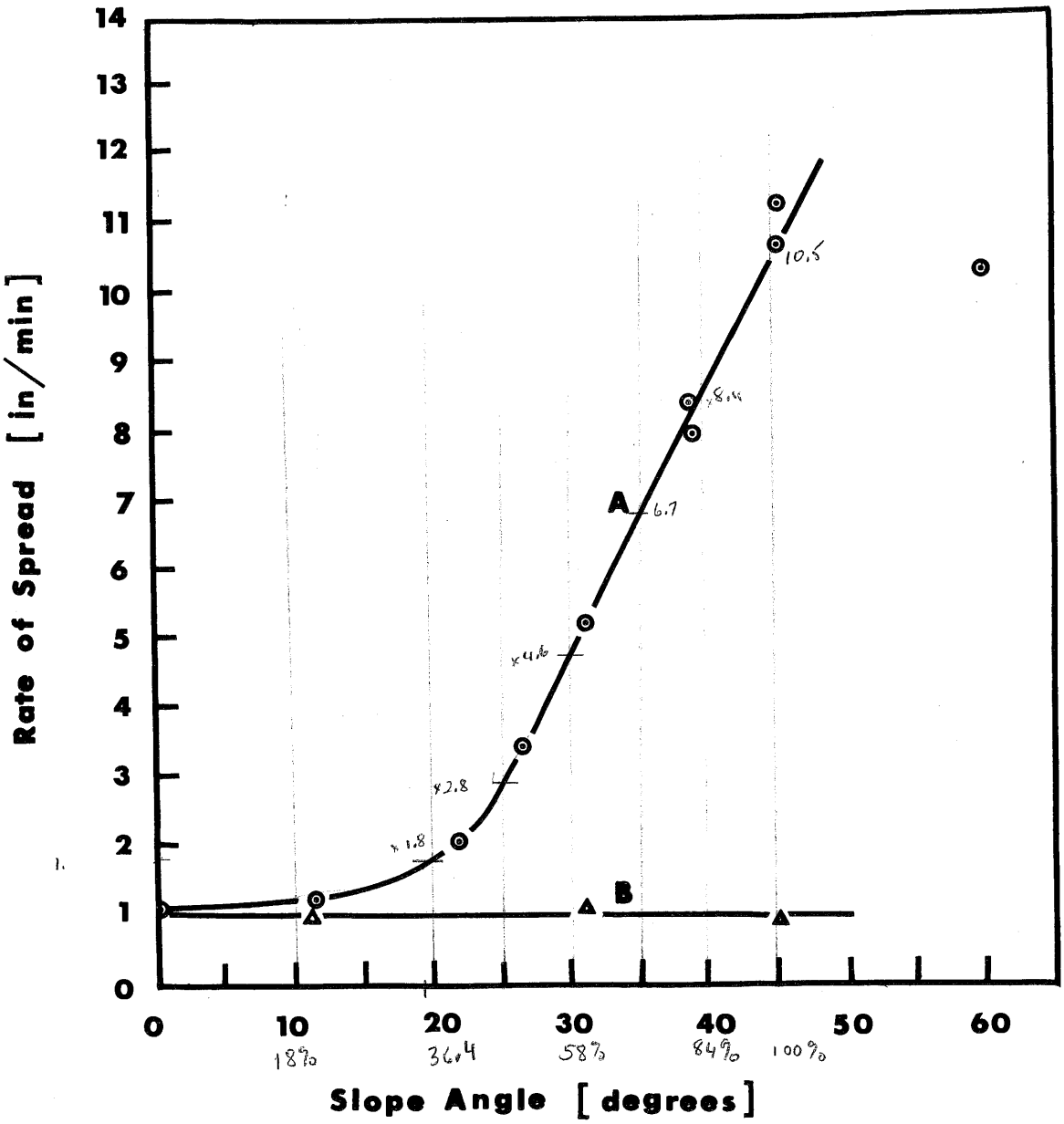

Figure 9.--The rate of spread for both upslope fires (curve A) and downslope fires (curve B) is shown as a function of the slope angle.

increases sharply when the slope angle exceeds 20°. The rate of spread of downslope fires is nearly independent of the slope angle; in this case the spread mechanism should be the same as for backfires in wind.

The diagram in Figure 10 corresponds to that in Figure 8. The line drawn through the plotted points has a slope of 1.0. Thus it would appear that t_r is essentially independent of slope angle, as it was of wind speed. Likewise, values of G and I_a based on Equations (4) and (5) would be independent of slope. Probably the burnout time τ is also independent of slope. However, further tests are needed to determine the slopes of the lines in Figures 8 and 10 more precisely. Also, the experiments should be repeated with other types of fuel beds. It may be that in general there is a slight dependence of t_r and τ on wind speed and slope angle.

It should be pointed out that the linear relationships shown in Figures 8 and 10 should break down as either the wind speed or slope angle approaches zero. The angle θ in the diagram of Figure 6 then approaches $\pi/2$ and the calm air spread mechanism takes over.

VARIATIONS IN THE UNIT AREA BURNING RATE ACROSS THE BURNING ZONE

The most useful form of the unit area burning rate is either its average value across the burning zone, which is given by Equations (2) and (3), or its average value across the flame zone as given by Equations (4) and (5). However, it is desirable to have some idea of the variation of the unit area burning rate across the burning zone

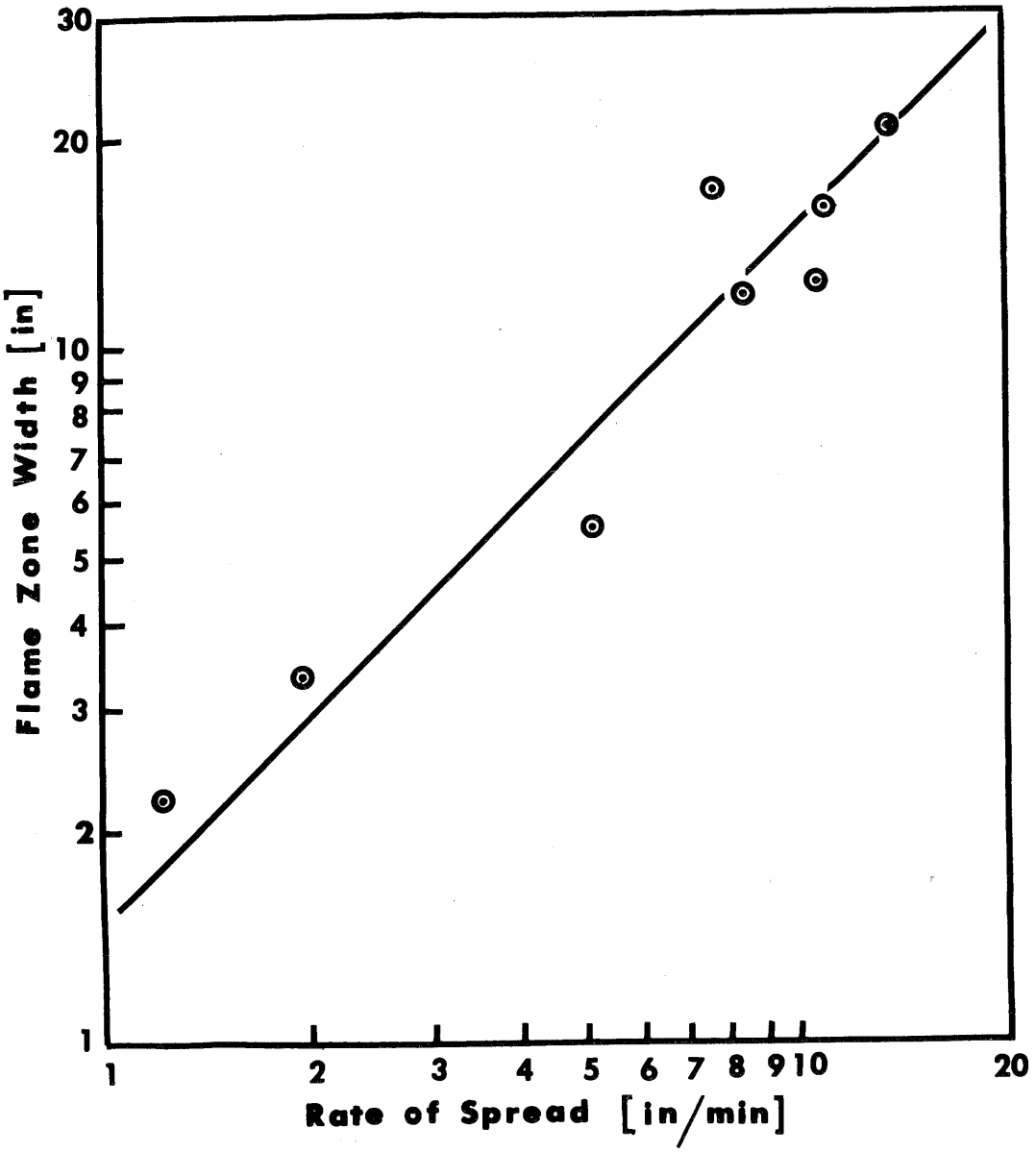

Figure 10.--The flame zone width D_z is shown as a function of the rate of spread R on a log-log plot for wood crib fires burned up sloping surfaces.

(which also includes the flame zone). To obtain an estimate of the variations in G across the burning zone for a slope fire, a crib on a 45° slope was allowed to burn to near completion and was then quickly extinguished. The remains of the crib were examined and weighed section by section. A similar test was made with the same type of crib in a wind stream of 5 ft/sec on a level surface. Both cribs were 6 feet long and their structure was identical to that of the cribs used in the wind and slope fires discussed in the two preceding sections.

Both fires were started by igniting an asbestos wick soaked with gasoline placed under one end of the crib. The slope fire was extinguished with a CO_2 fire extinguisher and the fire in wind by a low-velocity water mist. The water mist was more effective than the CO_2 gas and brought about extinguishment in just a few seconds without any tendency for re-kindling in the crib. The remains of each crib were divided into three separate zones. The first was composed mostly of ash and residual unburned charcoal. The second consisted of a mixture of charcoal and charred wood and the third zone was unburned crib. The first two zones were carefully cut into strip samples 1.25 inches wide and perpendicular to the length of the crib. They were oven-dried at a temperature of 220°F.

Curve A in Figure 11 shows how the weight loss of the strips for the slope fire varies with the distance from the leading edge of the flame zone. Curve B represents the slope of curve A and has the same dimensions as bulk crib density although the units for curve B

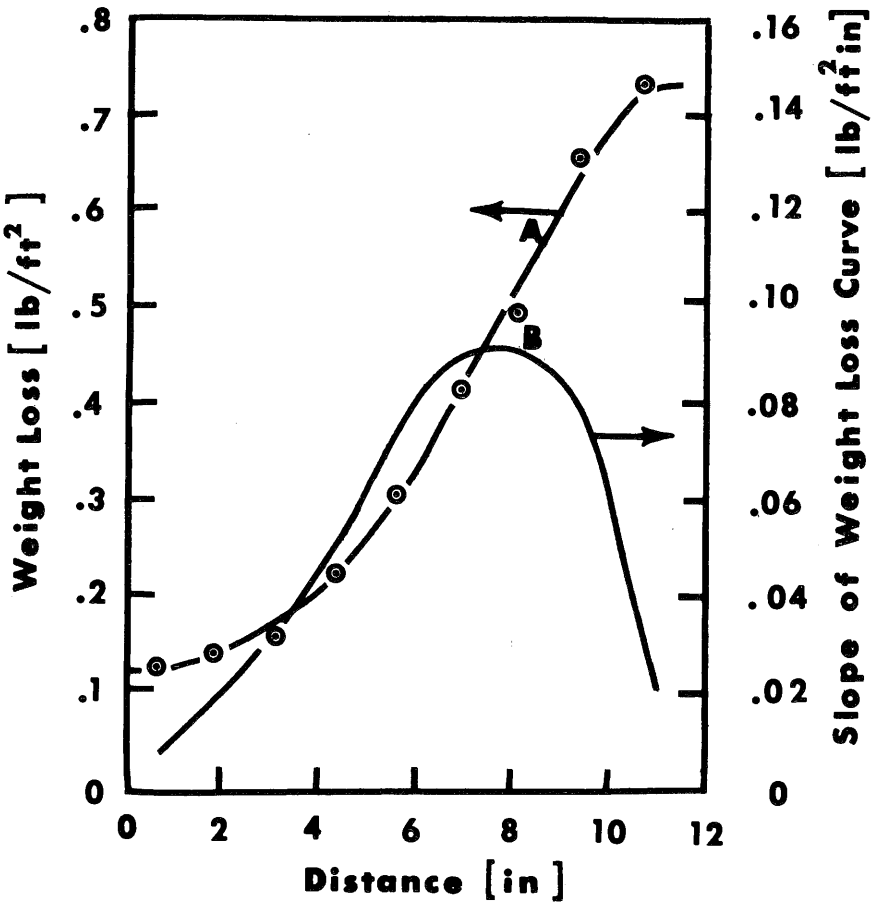

Figure 11.--Curve A shows the crib weight loss (lb/ft^2) for the slope fire as a function of the distance from the leading edge of the flame zone. Curve B represents the slope of curve A.

are lb/ft^2in. Multiplying the ordinates of curve B by the rate of spread R in in/min gives the local unit area burning rate G in lb/ft^2min for any given point in the burning zone. Figure 12 shows the corresponding curves for the fire in wind.

Although both fires had about the same rate of spread, approximately 3.5 in/min, there is considerable difference in the shape of the curves in Figure 11 compared to those in Figure 12. However, part of this difference may be due to the different method of extinguishment for the two fires because there was some difficulty with re-kindling for the slope fire and the extinguishment was slower. The maximum rate of weight loss was about 0.32 lb/ft^2min for the slope fire and about 0.34 lb/ft^2min for the fire in wind. Both of these maximum rates occurred at about the same distance from the leading edge of the burning zone but the burning zone width was considerably greater for the wind fire.

MOISTURE CONTENT AND FIRE SPREAD

Fuel moisture content and its effect on fire spread will be the only fuel property-fire spread relationship considered in this report. The wide fluctuations in the moisture content for wildland fuels, as well as the pronounced effect of moisture on fuel flammability and burning rate, make moisture content one of the key variables in the spread and behavior of all forest and wildland fires. For this reason, it seemed desirable to extend the results reported by Fons et al. (1962) in Summary Progress Report-II for crib fires to moisture contents high enough to approach the critical, or fire extinction, value.

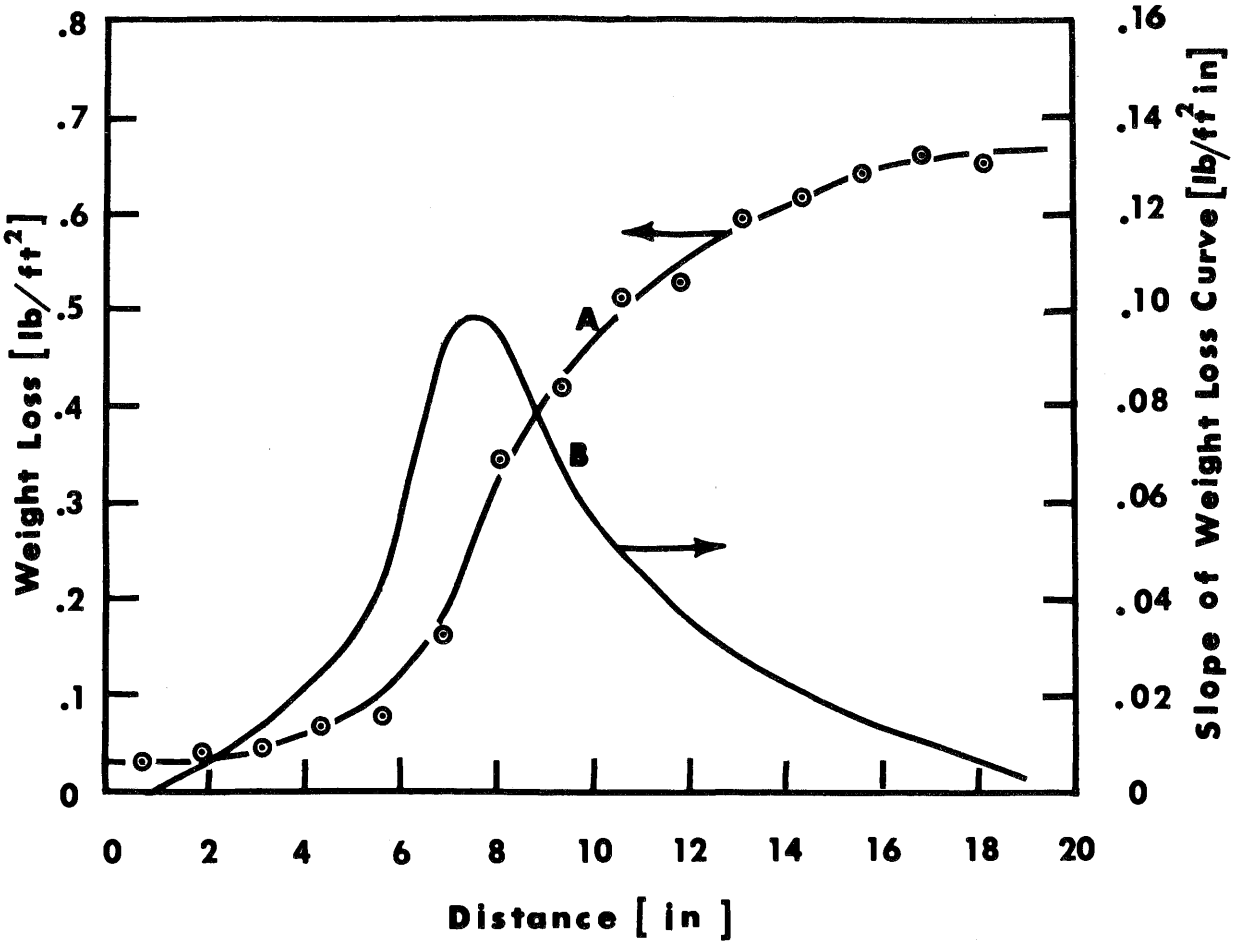

Figure 12.--Curve A shows the crib weight loss (lb/ft^2) for the fire in wind as a function of the distance from the leading edge of the flame zone. Curve B represents the slope of curve A.

The cribs were the same type used by Fons et al. (1962) and were 5.5 inches high and 9.25 inches wide. They were constructed from 0.44-inch square sticks of white fir with a lateral spacing of 1.25 inches. Three of the cribs were constructed from wood having a density of 24.0 lb/ft^3 and the rest from wood having a density of 28.6 lb/ft^3.

The cribs were conditioned in a constant-humidity cabinet to a moisture content of 11 percent and then weighed. After calculation of the bone-dry weights of the cribs from their known weights and moisture content, they were soaked in a tank of water until each had absorbed a quantity of water slightly in excess of that required for the desired moisture content. The cribs were then air dried to moisture contents of approximately 22, 37, and 50 percent and stored over water in a humidity cabinet until the time of burning. Fungal growth in the wood during storage was prevented by placing a small beaker of formaldehyde in the humidity cabinet.

In the first test, difficulty was experienced in igniting the crib directly with gasoline in a shallow trough. This was overcome by placing a short (5- to 6-inch) section of a low moisture content crib in front of the test crib. The short section was ignited and the fire spread into the higher moisture content test crib with a marked reduction in the burning rate. Once ignited, the test cribs burned at a slow but steady rate. Owing to the low rate of fire spread, steady-state burning was established after the fires had spread only a few inches. Figure 13 shows how the rate of fire spread in calm air varies with moisture content for the two

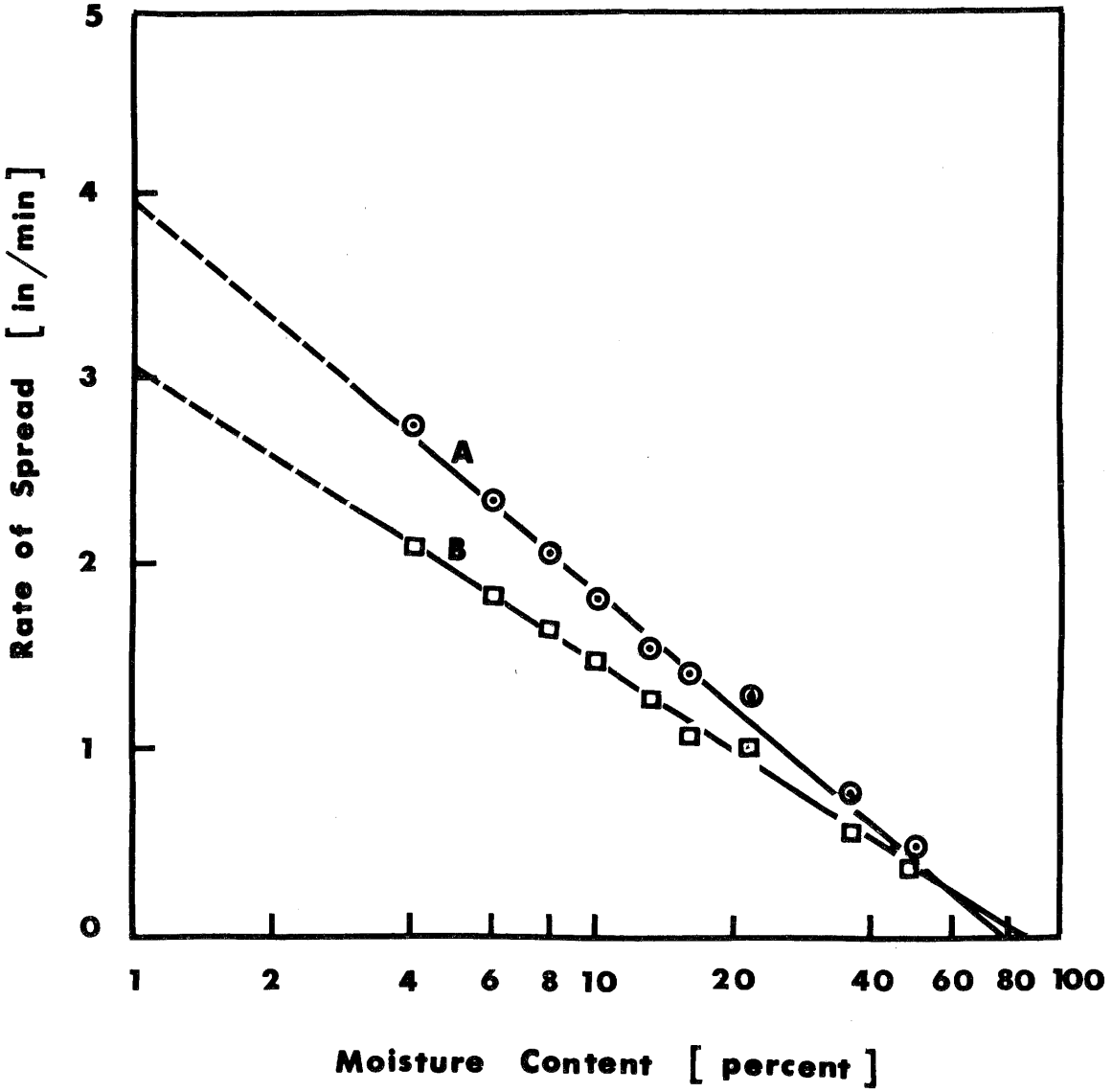

Figure 13.--The relationship between rate of fire spread and fuel moisture content for cribs with a density of 24.0 lb/ft^3 (curve A) and 28.6 lb/ft^3 (curve B).

different wood densities. For moisture contents of 16 percent and lower the points on the curves were interpolated from the results reported in Summary Progress Report-II. The curves can be represented to a close approximation by the equation

$$R = -K \log M/M_{cr}$$

where K is a constant with the dimensions of velocity and M_{cr} is the critical moisture content at which fire spread ceases. This equation is not valid for moisture contents approaching zero percent because R remains finite when M approaches zero. The constant K has a value of 0.90 in/min for cribs with a density of 24.0 lb/ft^3 and a value of 0.70 in/min for cribs with a density of 28.6 lb/ft^3. The intersection of curves A and B with the M-axis gives values of 78 and 84 percent for M_{cr} at these two densities.

It is very likely that the value of M_{cr} would be greater for crib headfires in wind than for fires in still air. Also, M_{cr} probably depends on crib structure, crib size, and the wood properties. If the cribs were burned in wind, K would become a variable strongly dependent on wind speed for headfires. It should also be influenced by the same variables and properties which affect M_{cr}. The effect of slope on M_{cr} and K should be similar to that of wind.

SCALING LAWS FOR FIRE MODELING

Test fires with wood cribs indicate that both slope and wind speed (variables which have a marked effect on rate of fire spread) may have only a minor influence on such important fuel variables as either the residence time or the fuel bed burnout time, as well as

the unit area burning rate of the fuel bed. The burnout time and the unit area burning rate also have a pronounced effect on rate of spread but their values are determined primarily by quantities associated only with the fuel bed such as fuel bed geometry, fuel moisture, and other fuel properties.

If it is found that the unit area burning rate and the fuel bed burnout time are essentially independent of wind speed and slope for other types of fuel beds, the problem of fire modeling will become much simpler; it should then be possible to consider it as two separate problems. One would constitute a study of the effect of wind and slope on fire spread. The only fuel variables entering this study would be the burnout time and unit area burning rate of the fuel bed, although there are equivalent alternate pairs of fuel variables which could also be used. The other problem would be a study of the relation of the burnout time and unit area burning rate to fuel bed geometry, fuel moisture, and other fuel properties. The methods of modeling may not be as well suited to this problem as to the first.

Work on the first problem is now underway and considerable progress has been made in developing the scaling laws needed for modeling fire spread in wind and on sloping surfaces. The more important dimensionless groups and the resulting scaling laws are summarized briefly in the following paragraphs for fires in wind but their derivation and development will not be given in this report.

Although many variables are involved in the behavior of both moving fires and stationary fires, a dimensional analysis shows that

these fires can be characterized by a relatively few types of dimensionless groups. These are represented by the symbol π in the following tabulation

$$\pi_1 = v/(gx)^{\frac{1}{2}} \qquad \pi_3 = t(g/x)^{\frac{1}{2}}$$

$$\pi_2 = \frac{I_a/(gx)^{\frac{1}{2}}}{\rho c_p T_o} \qquad \pi_4 = z/x$$

$$\pi_5 = vx/\nu$$

in which π_1 is a Froude number, π_2 can be defined as a buoyancy number, π_3 is the square root of an acceleration ratio, π_4 is a length ratio, and π_5 is a Reynolds number. In the Froude number, v represents any velocity such as wind velocity, indraft velocity, or updraft velocity in the convection column. If information is desired on each of these velocities, there must be three Froude numbers in the analysis. The length x is a characterizing dimension of the burning area and g the acceleration due to gravity. In the buoyancy number, I_a is the unit area burning rate (expressed as the rate of convective heat output per unit area of source) and ρ , c_p, and T_o are the density, specific heat at constant pressure, and absolute temperature of the environmental air. In the acceleration ratio, t represents any time variable. In the group π_4 , the length z represents any length variable associated with either the flame, convection column, or fuel bed. In the Reynolds number, ν can be taken as either the kinematic viscosity of the environmental air or that of the flame and convection column gases.

Scaling laws for modeling are determined by giving each π the same value for both the model and full-scale fire. However, in the case of the Reynolds number this procedure results in a scaling relationship which is not consistent with those given by the other groups if both the model and the full-scale fire burn in air. This indicates that the model must be large enough for viscous forces to be disregarded, in which case the Reynolds number would be large enough to drop. If the Reynolds number is dropped and if π_1, π_2, π_3, and π_4 are each given the same value for the model as for the full-scale fire, then the resulting scaling relationships are

$$\frac{v_m}{v_f} = \frac{(I_a)_m}{(I_a)_f} = \frac{t_m}{t_f} = (x_m/x_f)^{\frac{1}{2}} \tag{6}$$

and

$$\frac{z_m}{z_f} = \frac{x_m}{x_f} \tag{7}$$

where the subscripts m and f denote model and full scale, respectively. The variables in Equation (6) scale as $x^{\frac{1}{2}}$ and Equation (7) shows that all lengths scale directly as x. Hence the full-scale fire and its model are geometrically similar.

For a fire or heat source in the form of an infinitely long strip of width x, the groups π_1 and π_2 can be combined to give the relationship

$$\pi_6 = \frac{gI}{\rho c_p T_o v^3}$$

in which $I = I_a x$ and is the rate of convective heat output per unit

length of the strip source. The π_6 group may be defined as a convection number. If z is taken as the height of any point in the convection column, then in that region of the column for which $z \gg x$, the angle of tilt of the column is determined by the value of π_6.

For an area source I is the total rate of convective heat output, hence $I \propto I_a x^2$. In this case the combining of π_1 and π_2 gives

$$\pi_7 = (g^2 I)/ \rho c_p T_o v^5$$

where π_7 is the convection number for an area source corresponding to π_6 for the strip source.

Scaling laws for I for a strip source and an area source are (from π_6 and π_7)

$$\frac{v_m}{v_f} = (I_m/I_f)^{1/3}$$

for the strip source and

$$\frac{v_m}{v_f} = (I_m/I_f)^{1/5}$$

for the area source. On comparing these equations with Equations (6) it follows that

$$\frac{I_m}{I_f} = (x_m/x_f)^{3/2}$$

for the strip source and

$$\frac{I_m}{I_f} = (x_m/x_f)^{5/2}$$

for the area source.

Model fires which meet the requirements of the scaling laws will be considerably different than those used in past work. For example, the rates of spread of such fires would be many times as great as that for the crib fires described in this report. However, both the unit area burning rate and fuel loading would be much less than for the crib fires. The effects of viscous forces on model fires have not yet been determined but it is possible that their influence may require considerably larger fires than those used in past studies.

REFERENCES

Anderson, H. E., and Rothermel, R. C.
1965. Influence of Moisture and Wind upon the Characteristics of Free-burning Fires. Tenth Symposium (International) on Combustion, p. 1009, The Combustion Institute, Pittsburgh, Pennsylvania.

Byram, G. M., Clements, H. B., Elliott, E. R., and George, P. M.
1964. An Experimental Study of Model Fires. Technical Report No. 3. U. S. Forest Serv., Southeastern Forest Expt. Sta. 36 pp.

Curry, J. R., and Fons, W. L.
1938. Rate of Spread of Surface Fires in the Ponderosa Pine Type of California. Jour. Agr. Res. 57: 239-267.

Fons, W. L.
1946. Analysis of Fire Spread in Light Forest Fuels. Jour. Agr. Res. 72: 93-121.

_____ Clements, H. B., Elliott, E. R., and George, P. M.
1962. Project Fire Model, Summary Progress Report - II. U. S. Forest Serv., Southeastern Forest Expt. Sta., 55 pp.

McAdams, W. H.
1954. Heat Transmission. 3rd ed., p. 259, McGraw-Hill Book Co., Inc., New York.

Moffat, R. J.
1962. Gas Temperature Measurement. Temperature - Its Measurement and Control in Science and Industry, Part 2, p. 553, Reinhold Pub. Corp., New York.

Murphy, P. J.
1963. Rates of Fire Spread in an Artificial Fuel. Master's Thesis, Montana State University. 90 pp.

APPENDIX A

CORRECTIONS FOR FLAME TEMPERATURE MEASUREMENTS

There is considerable information available in the literature on the corrections for thermocouple measurements of the temperature of hot gases. Ordinarily, these corrections are difficult to make and may be subject to error as pointed out by Moffat (1962). However, for thermocouples made of fine wire, the heat loss resulting from conduction along the wire is small compared to the radiation loss. Furthermore, the problem of flame temperature measurement is simplified if the temperature of the surfaces in the environment surrounding the flame is low. One term in the heat balance equation is eliminated if it can be assumed that the flame is small. A "small" flame will be defined as one for which the rate at which the thermocouple receives heat from the flame by radiation is small compared to the rate at which the thermocouple loses heat by radiation. In this case, the thermocouple would receive substantially all of its heat by convection and conduction from the flames. Probably, laboratory fires of the size discussed in this report can be considered "small" but the assumption should not be valid for the flames of extensive high-intensity fires in the field. Thermocouple readings in large flames would tend to approach the actual flame temperature.

If the loss of heat by conduction along the thermocouple wire is neglected, the heat balance equation for a small flame has the simplified form

$$h(T_f - T_{th}) = \sigma e \, (T_{th}^4 - T_o^4) \qquad \text{(A-1)}$$

in which h is the convective heat transfer coefficient, e the thermocouple emissivity, σ the Stefan-Boltzmann constant, and T_f, T_{th}, and T_o, are the absolute temperatures of the flames, thermocouple, and surrounding surfaces, respectively.

The convective heat transfer coefficient h is given by an equation involving a relationship between the Nusselt number and the Reynolds number. This relationship is

$$\frac{hd}{k} = F\left(\frac{ud}{\nu}\right), \qquad \text{(A-2)}$$

where d is the diameter of the thermocouple wire, k the thermal conductivity of air at the film temperature $\frac{1}{2}(T_f + T_{th})$, ν the kinematic viscosity of air at the film temperature, and u is the gas velocity. The function F depends on the orientation of the thermocouple wire (cylinder) with respect to the direction of gas flow. McAdams (1954) gives a graphical representation of Equation (A-2) for air flowing normal to single cylinders. This curve and Equation (A-1) can be used to make estimates of the true flame temperature from bare thermocouple readings and measurements of the gas velocity. Since the thermal conductivity and kinematic viscosity of the flame gases are not known, it will be assumed that the corresponding properties for air at the same temperature can be substituted without introducing an appreciable error.

The method used for estimating the true flame temperature is given in the following procedure:

1. Determine the thermocouple reading T_{th}.

2. Determine the flame velocity u. If a Prandtl tube is used, correct the indicated velocity to the air density corresponding to T_{th} (air density is used because the density of the flame gases is not known). This correction is equivalent to multiplying the indicated velocity by $(T_{th}/T_o)^{\frac{1}{2}}$.
3. Using the corrected value of the gas velocity u and using a value of the kinematic viscosity ν based on T_{th}, compute the Reynolds number and determine the corresponding value of the Nusselt number from graphical or tabulated values of the function in Equation (A-2).
4. Using a value of k based on T_{th}, compute h from the Nusselt number.
5. Compute the first approximation of T_f from Equation (A-1).
6. Make a second approximation of u in step 2 based on the temperature $\frac{1}{2}(T_f + T_{th})$ instead of T_{th}.
7. Repeat steps 3 and 4 with the temperature $\frac{1}{2}(T_f + T_{th})$ substituted for T_{th} and obtain a second approximation of h.
8. Use Equation (A-1) to obtain a second approximation of T_f.
9. Repeat the procedure until the difference between successive approximations is within the desired limit of error. Usually only two or three approximations are necessary.

A thermocouple which indicates a temperature in the neighborhood of 1800°F in the flames of a small fire is probably reading from 300 to 500°F too low.

APPENDIX B

BASIC DATA FROM TEST FIRES

Tables 1 to 6 give the experimental conditions and results of tests with pool and crib fires. The pool fire data in Table 1 were obtained with vertical glass panels placed at the sides of the pools. The panels were mounted parallel to the direction of the air flow.

The fires for Tables 2 and 3 burned in calm air. The corrected flame temperatures were obtained by the procedure described in Appendix A.

In Table 5, fires S-4R and S-5R are repeat tests of fires S-4 and S-5. Fire F-30 appears both in Table 4 and Table 5.

The cribs for the fires in Table 6 were the same type used by Fons et al. (1962) in similar tests which had been made at lower moisture contents.

In converting mass burning rates to heat output rates for small fires in woody fuels, the convective heat of combustion may be taken as approximately 75 percent of the low heat value for moisture contents up to 15 percent of the bone-dry weight of the fuel. The 75 percent approximation may also be used for ethanol.

The average low heat value for a wide range of woods and woody substances is about 8600 Btu/lb. Fons et al. (1962) give a value of 8135 Btu/lb for white fir (Abies concolor) crib material such as was used in this study.

Table 1.--Data for ethanol pool fires burned in wind.

Fire No.	Wind speed	Fuel pan width	Ignition distance	Scorch distance	Horizontal flame length	Unit area burning rate
	ft/sec	in	in	in	in	lb/ft^2 min
WP-4	2.0	2.5	18.0	9.7	8.3	0.19
WP-5	4.3	2.5	18.0	9.7	8.8	0.19
WP-6	6.1	2.5	17.0	9.7	9.7	0.18
WP-7	7.9	2.5	22.5	13.0	12.0	0.19
WP-8A	10.1	2.5	28.0	14.5	13.4	0.20
WP-9	2.0	5.0	24.0	14.2	13.0	0.18
WP-10	4.3	5.0	28.0	14.1	14.6	0.18
WP-11	6.1	5.0	24.0	15.4	15.0	0.16
WP-12	7.9	5.0	36.0	23.1	17.1	0.17
WP-13	10.1	5.0	38.0	20.5	17.2	0.16
WP-14	2.0	12.8	29.0	18.1	16.7	0.18
WP-15	4.3	12.8	39.0	24.7	22.9	0.17
WP-16	6.1	12.8	42.0	24.2	25.4	0.15
WP-17	7.9	12.8	48.0	27.3	25.4	0.12
WP-18	10.1	12.8	54.0	31.2	28.0	0.11

Table 2.--Flame temperatures and central vertical velocities for 12.8-inch pool fires of burning ethanol at different heights above the pool surface.

Fire No.	Height above fuel	Flame gas velocity	Thermocouple temperature	Corrected flame temperature	Temperature difference
	in	ft/sec	°F	°F	°F
TP-1	2	6.8	1265	1468	203
TP-2	4	11.1	1492	1765	273
TP-3	6	11.4	1681	2073	392
TP-4	8	13.1	1794	2252	458
TP-5	10	13.6	1749	2169	420
TP-6	12	13.3	1703	2087	384
TP-7	16	13.5	1547	1833	286
TP-8	20	12.4	1350	1546	196
TP-9	24	13.9	1222	1362	140
TP-10	30	11.4	788	834	46

Table 3.--Flame temperatures and central vertical flame velocities for white fir (Abies concolor) crib fires at different heights above the crib surface. Each crib was 11.6 inches square and 1.56 inches high and was constructed from 0.256-inch sticks.

Fire No.	Height above fuel	Flame gas velocity	Thermocouple temperature	Corrected flame temperature	Temperature difference
	in	ft/sec	°F	°F	°F
TW-1	48	8.1	252	256	4
TW-2	42	15.0	671	698	27
TW-3	36	22.2	841	882	41
TW-4	30	24.9	1351	1499	148
TW-5	24	22.8	1265	1391	126
TW-6	18	19.7	1329	1483	154
TW-7	16	19.0	1547	1796	249
TW-8	12	25.8	1658	1929	271
TW-9	8	18.4	1681	2007	326
TW-10	6	22.5	1840	2240	400

Table 4.--Crib characteristics, atmospheric conditions, and experimental results for cribs burned in wind. The cribs were made from 0.256-inch white fir (Abies concolor) sticks with a 1.0-inch spacing. Each crib was 1.56 inches high and 11.6 inches wide. Headfires are identified by "F" and backfires by "FB." Air temperatures for all fires were in the range 69 to 74°F and relative humidities in the range 54 to 62 percent.

Fire No.	Wood density	Crib weight	Crib length	Moisture content	Wind speed	Rate of spread		Flame zone width
						Front	Rear	
	lb/ft^3	lb	in	percent	ft/sec	in/min	in/min	in
F-20	25.6	3.89	71.8	10.9	2.0	2.15	2.18	7.0
F-21	25.8	3.91	71.8	10.9	3.0	2.60	2.53	7.0
F-22	25.8	7.81	143	10.9	5.0	3.51	3.56	10.6
F-23	25.8	9.78	180	10.7	8.0	6.41	6.58	19.5
F-24	25.8	9.79	180	10.7	10.0	9.61	8.33	40.5
F-25	25.9	3.93	71.8	10.4	2.0	2.43	2.50	7.5
F-26	25.9	3.93	71.8	10.4	3.0	2.47	2.60	7.2
F-27	26.0	5.93	108	10.4	5.0	3.47	3.51	10.0
F-28	25.9	9.80	180	10.4	8.0	6.00	6.15	19.2
F-29	25.9	13.71	251	10.4	12.0	11.4	11.4	33.0
F-30	26.1	2.03	36.7	10.9	0.0	1.09	--	4.1
F-31	25.8	9.76	180	11.0	10.0	8.90	8.70	31.5
FB-32	25.8	1.98	36.4	11.4	-2.0	1.15	1.20	3.1
FB-33	25.6	1.95	36.4	11.4	-5.0	1.20	1.31	2.7
FB-34	26.3	2.01	36.4	11.4	-12.0	1.32	1.26	2.3
FB-35	25.8	1.98	36.4	11.3	-8.5	1.42	1.44	1.8

Table 5.--Crib characteristics, atmospheric conditions, and experimental results for cribs burned on sloping surfaces. Cribs were made of 0.256-inch white fir sticks (Abies concolor) with a 1.0-inch spacing. The cribs were 1.56 inches high and 11.6 inches wide. Upslope fires are identified by "S" and downslope fires by "SB." Air temperatures for all fires were in the range 71 to 84°F and relative humidities in the range 54 to 62 percent.

Fire No.	Wood density	Crib weight	Crib length	Moisture content	Slope angle	Rate of spread		Flame zone width
						Front	Rear	
	lb/ft^3	lb	in	percent	degrees	in/min	in/min	in
S-1	26.1	3.93	71.6	11.0	11.3	1.22	1.21	2.2
S-2	26.0	3.91	71.6	11.0	21.8	1.95	2.00	3.4
S-3	26.0	3.91	71.6	11.2	31.0	5.06	5.20	5.5
S-4	26.1	5.93	108	11.2	38.7	7.57	8.17	17.0
S-5	25.8	5.86	108	11.0	45.0	10.6	10.6	12.5
S-6	25.7	5.84	108	11.0	60.0	13.5	7.05	21.0
S-4R	26.1	5.92	108	11.0	38.7	8.35	8.30	12.0
S-5R	26.0	5.88	108	11.3	45.0	10.9	11.5	16.0
SB-1	26.0	1.98	36.4	11.4	11.3	0.96	.98	1.7
SB-2	25.8	1.97	36.4	11.4	31.0	1.03	1.04	3.0
SB-3	25.8	1.97	36.4	11.1	45.0	0.93	.92	2.9
F-30	26.1	2.03	36.7	10.9	0.0	1.09	--	4.1

Table 6.--Crib characteristics, atmospheric conditions, and experimental results for cribs burned at high moisture contents. Cribs were 9.25 inches wide and 5.5 inches high. They were made of 0.44-inch white fir (Abies concolor) sticks spaced at 1.25 inches.

Fire No.	Wood density	Crib weight	Crib length	Moisture content	Rate of spread
	lb/ft^3	lb	in	percent	in/min
99	28.2	7.22	35.5	22.2	0.98
100	23.4	5.98	35.5	22.2	1.26
101	28.8	3.85	19.3	37.5	0.57
102	24.3	3.23	19.1	36.4	0.73
103	24.3	2.83	16.4	50.4	0.47
104	29.0	3.38	16.4	49.7	0.34

DISTRIBUTION LIST

No. of Copies

Dept. of the Army (55)
Off. of Civil Defense, OSA
Washington, D. C. 20310
Attn: A/Director of Civil Defense, Research

Dept. of the Army (3)
Off. of the Adjutant General
Washington, D. C. 20310
Attn: AGAL-CD

Defense Documentation Center (20)
Cameron Station
Alexandria, Virginia 22314

Weapons Systems Evaluation Group (1)
Department of Defense
Washington, D. C. 20301
Attn: Library

Weapons Systems Evaluation Group (1)
Dept. of Defense
Rm. 2E812, The Pentagon
Washington, D. C. 20301

ARPA (1)
Dept. of Defense
Washington, D. C. 20301
Attn: Chief, Missile Phenomenology Branch
Rm. 3D156, The Pentagon

ARPA/AGILE (1)
Dept. of Defense
Washington, D. C. 20301
Attn: Dir. for Remote Area Conflict
Rm. 3E169, The Pentagon

ARPA/BMD (1)
Dept. of Defense
Washington, D. C. 20301
Attn: Chief, Mechanics Branch
Rm. 2B260, The Pentagon

Defense Intelligence Agency (DIAAF-1K2) (1)
Washington, D. C 20305

No. of Copies

Defense Atomic Support Agency (1)
The Pentagon
Washington, D. C. 20301
Attn: Thermal Effects Branch

Defense Atomic Support Agency (1)
The Pentagon
Washington, D. C. 20301
Attn: Technical Library

Commander, Field Command (1)
Defense Atomic Support Agency
Sandia Base
Albuquerque, New Mex.
Attn: Tech. Library

Asst. Secretary of the Army (R&D) (1)
Washington, D. C. 20310
Attn: Asst. for Research

Joint Civil Def. Support Group (1)
Off. of the Chief of Engineers
Dept. of the Army
Gravelly Point, Virginia 20315

U. S. Army Engineers R&D Lab. (1)
Fort Belvoir, Va. 22060
Attn: Tech. Library

The Engineer School (1)
Fort Belvoir, Va. 22060
Attn: Library

Army War College (1)
Carlisle Barracks, Pa.
Attn: Library

The War College (1)
Fort McNair
Washington, D. C. 20315
Attn: Library

U. S. Army Engineers R&D Lab. (1)
Fort Belvoir, Va. 22060
Attn: Chief, Fire Suppression Sec.
Sanitary Sciences Branch

Chief, NMCSSC (1)
Rm. BE 685 (Code B210) The Pentagon
Washington, D. C. 20301

U. S. Army Nuclear Defense Laboratory (1)
Edgewood, Maryland 21040
Attn: Technical Library

U. S. Naval Applied Science Laboratory (1)
Brooklyn, New York 11251
Attn: Technical Library

U. S. Naval Applied Science Laboratory (1)
Brooklyn, New York 11251
Attn: Mr. Willard Derksen

U. S. Naval Civil Engineering Laboratory
Port Hueneme, Calif. (1)
Attn: Technical Library

U. S. Naval Radiological Defense Lab. (1)
San Francisco, Calif. 94135
Attn: Technical Library

U. S. Naval Radiological Defense Lab. (1)
San Francisco, Calif. 94135
Attn: Mr. Stanley Martin

U. S. Naval Radiological Defense Lab. (1)
San Francisco, Calif. 94135
Attn: Dr. M. G. Gibbons (Code 912)

U. S. Naval Research Laboratory (1)
Washington, D. C. 20390
Attn: Technical Library

U. S. Naval Research Laboratory (Code 6220)
Washington, D. C. 20390 (1)
Attn: Mr. Richard E. Tuve

Chief, Bureau of Medicine & Surgery (1)
Department of the Navy
Washington, D. C. 20390

Chief, Bureau of Supplies & Accounts (1)
(Code L 12)
Department of the Navy
Washington, D. C.

Chief of Research & Development (1)
Hdqtrs., Dept. of the Army
Washington, D. C. 20310
Attn: Atomic Office

Chief, Bureau of Naval Weapons (1)
(Code RRRE-5)
Department of the Navy

Chief, Bureau of Ships (Code 203) (1)
Department of the Navy
Washington, D. C.

Chief of Naval Research (Code 104)(1)
Department of the Navy
Washington, D. C.

Chief, Bureau of Naval Operations (1)
(Op 07T10)
Department of the Navy
Washington, D. C.

Director, Special Projects Office (1)
(Code SP-114)
Department of the Navy
Washington, D. C.

Coordinator, Marine Corps Landing Force
Development Activities (1)
Quantico, Virginia

Asst. Secretary of the Air Force (R&D)
The Pentagon, Rm. 4E962
Washington, D. C. 20330 (1)

Hdqtrs., U. S. Air Force (AFGOA) (1)
Washington, D. C. 20330

Director, U. S. Air Force R & D (1)
Office of Scientific Research
Tempo D, 6th & Indep. Ave., S.W.
Washington, D. C. 20333
Attn: Technical Library

U. S. Air Force Special Weapons Center
Kirtland Air Force Base (1)
Albuquerque, New Mexico
Attn: Library

Chief, Bureau of Yards and Docks (1)
Office of Research (Code 74)
Department of the Navy
Washington, D. C.

Air Force Aero Propulsion Laboratory (1)
Aeronautical Systems Division
Wright-Patterson Air Force Base
Dayton, Ohio
Attn: Mr. B. Botteri

U. S. Atomic Energy Commission (1)
Washington, D. C. 20545
Attn: Technical Information Service

U. S. Atomic Energy Commission (1)
Washington, D. C. 20545
Attn: Headquarters Report Library
G-017

U. S. Atomic Energy Commission (1)
Washington, D. C. 20545
Attn: Div. of Biology & Medicine
E-201

Director, Div. of Forest Fire Research (1)
U. S. Dept. of Agriculture
Forest Service
Washington, D. C. 20250

U. S. Dept. of Agriculture (1)
Intermountain Forest & Range Exp. Sta.
Missoula, Montana
Attn: Forest Fire Research

U. S. Dept. of Agriculture (1)
Pacific Southwest Forest & Range Exp. Sta.
P. O. Box 245
Berkeley, Calif. 94701

U. S. Dept. of Agriculture (1)
Forest Service
Southern Forest Fire Laboratory
P. O. Box 236, Macon, Ga. 31202

National Academy of Sciences (11)
National Research Council
Committee on Fire Research
2101 Constitution Ave., N. W.
Washington, D. C. 20418

Air University (1)
Maxwell Air Force Base
Alabama
Attn: Library

Mr. Gifford Cook, Deputy Chief (1)
Fire Protection Group
Headquarters, US Air Force
AFOCE-D
Washington, D. C. 20330

Nat'l. Academy of Sciences (1)
Advisory Committee on Civil Defense
2101 Constitution Ave., N. W.
Washington, D. C. 20418
Attn: Dr. Richard Park

Federal Fire Council (1)
Gen. Services Adm. Bldg. - Rm. 4311
19th & F. Sts., N. W.
Washington, D. C. 20405

U. S. Department of the Interior (2)
Bureau of Mines
Branch of Explosives Research
Washington, D. C. 20240

Dr. Walter G. Berl (1)
Applied Physics Laboratory
The Johns Hopkins University
8621 Georgia Avenue
Silver Spring, Maryland

U. S. Dept. of Interior (1)
Bureau of Mines
4800 Forbes Ave.
Pittsburgh, Pa. 13
Attn: Mr. R. W. Van Dolah

Woods Hole Institute of Oceanography
Woods Hole, Mass. (1)
Attn: Library

Institute for Defense Analysis (1)
400 Army-Navy Drive
Arlington, Va. 22202
Attn: Chief, EPS Division

Institute for Defense Analysis (1)
400 Army-Navy Drive
Arlington, Va. 22202
Attn: Library

National Science Foundation (1)
Director for Mathematical, Physical
& Engineering Sciences
Washington, D. C. 20550

Dr. Walter T. Olson (1)
Lewis Research Center
National Aeronautics & Space Adm.
21000 Brookpark Rd.
Cleveland, Ohio

Mr. C. M. Middleworth (1)
Systems Research & Devel. Service
Federal Aviation Agency
Natl. Aviation Facilities Exper. Center
Atlantic City, N. J.

ASHRAE Bibliographical Project (1)
New York University
Research Bldg. No. 1
University Heights
New York, New York
Attn: Mr. E. R. Kaiser

College of Engineering (1)
University of Florida
Gainesville, Florida
Attn: Civil Defense Library

University of Georgia (1)
Athens, Georgia
Attn: Civil Defense Library

University of California (San Diego) (1)
Dept. of Aerospace & Mechanical Eng. Sciences
P. O. Box 109
La Jolla, Calif.
Attn: Dr. Forman A. Williams

University of Md. (1)
Fire Service Extension
College Park, Maryland
Attn: Mr. Robt. C. Byrus, Director

Institute for Defense Analysis (1)
400 Army-Navy Drive
Arlington, Va. 22202
Attn: Chief, R&E Support Div.

University of Maryland (1)
Fire Protection Curriculum
College Park, Md.
Attn: Mr. John Bryan

Oklahoma State University (1)
Fire Protection Dept.
Technical Institute
Stillwater, Okla.
Attn: Mr. Elmer Johnson, Head

Illinois Institute of Technology (1)
Dept. of Fire Protection & Safety Engr.
Chicago, Ill. 60616
Attn: Mr. G. L. Maatman

Illinois Institute of Technology (1)
Research Institute
10 W. 35th St.
Chicago, Ill. 60616

The Johns Hopkins University (1)
Applied Physics Lab.
8621 Georgia Ave.
Silver Spring, Md.
Attn: Dr. Robert Fristrom

Mr. John Rhodes (1)
Director of Engineering & Research
Factory Mutual Engineering Division
1151 Boston-Providence Turnpike
Norwood, Massachusetts 02062

Georgia Instit. of Technology (1)
School of Industrial Engineering
Atlanta, Ga.
Attn: Prof. Wm. N. Cox, Jr.

Massachusetts Instit. of Technology
Cambridge, Mass. 02139 (1)
Attn: Prof. H. C. Hottel
Director, Fuels Research Lab.

Research Triangle Institute (1)
P. O. Box 490
Durham, North Carolina
Attn: Dr. Edgar A. Parsons

University of Maryland (1)
Engineering Library
College Park, Md.

System Development Corporation (1)
2500 Colorado Ave.
Santa Monica, Calif.
Attn: Dr. Hilton F. Jarrett

Bio-dynamics, Inc. (1)
One Main Street
Cambridge, Mass.
Attn: Mr. Robt. E. O'Brien, Pres.

Factory Mutual Research Corporation (1)
1151 Boston-Providence Turnpike
Norwood, Mass.
Attn: Mr. M. B. Smith, Vice-Pres.

American Insurance Assn. (1)
110 William St.
New York, N. Y. 10038
Attn: Dr. M. M. Braidech, Dir. of Research

Oak Ridge Natl. Laboratory (1)
Oak Ridge, Tenn.
Attn: Dr. Eugene Wigner

Dikewood Corporation (1)
4805 Menaul Blvd., N.E.
Albuquerque, New Mex.
Attn: Mr. Tom Lommasson

Lockheed Missiles and Space Co. (1)
Technical Information Center
3251 Hanover St.
Palo Alto, Calif.
Attn: Dr. R. Meyerott

Edgerton, Germeshausen & Grier, Inc. (1)
P. O. Box 384, Kenmore Station
Boston, Mass.
Attn: Civil Defense Library

Hudson Institute (1)
Quaker Ridge Road
Harmon-on-Hudson, New York 10520
Attn: Dr. William Brown

Dr. Howard W. Emmons (1)
Dept. of Mechanical Engineering
Harvard University
Cambridge, Mass. 02138

Dept. of Mechanical Engineering (1)
Instit. of Technology, U. of Minn.
Minneapolis, Minn. 55455
Attn: Prof. Perry L. Blackshear, Jr.

Natl. Fire Protection Assn. Library
60 Batterymarch St. (1)
Boston, Mass. 02110

Mr. George H. Tryon, Tech. Secretary
Natl. Fire Protection Assn. (1)
60 Batterymarch St.
Boston, Mass. 02110

Underwriters Laboratories, Inc. (1)
207 E. Ohio St.
Chicago, Ill. 60611
Attn: Library

Dr. Richard L. Tuve, Head (1)
Engineering Research Branch
Code 6220
U. S. Naval Research Laboratory
Washington, D. C. 20390

Dr. Edward E. Zukoski (1)
California Institute of Technology
Pasadena, California

Dr. Bernard Lewis (1)
Combustion & Explosives Research, Inc.
1007 Oliver Bldg.
Pittsburgh, Pennsylvania 15222

Dr. A. F. Robertson, Chief (25)
Fire Research Section
National Bureau of Standards
Washington, D. C. 20234

U. S. Natl. Bureau of Standards (1)
Office of Technical Information and Publications
Washington, D. C.

Stanford Research Institute (1)
Menlo Park, Calif. 94025
Attn: Director, Civil Defense Tech. Office